This article has been accepted for publication in a future issue of this journal, but has not been fully edited. Content may change prior to final publication. Citation information: DOI 10.1109/JSAC.2014.2332132, IEEE Journal on Selected Areas in Communications

Network Theory and Smart Grid Distribution Automation

Stephen F Bush, *Senior Member, IEEE*

***Abstract*—The communication network supports applications within the power grid that cannot be handled by local control; there is a mutual relationship that influences their network structures. This leads to the hypothesis that there is a fundamental relationship involving the eigenvalues of the power grid network and communication network adjacency matrices. The intuitive relationship is that the communication network adjacency matrix should have stronger connectivity among nodes that are weakly-connected in the power network adjacency matrix. The focus is upon latency rather than bandwidth since, in the application of fault detection, isolation, and recovery, messages are relatively small but their speed of transmission is of greater importance.**

***Index Terms*—Distribution automation, Communications, Network science, Computer network reliability, Wireless sensor networks, Power distribution faults, Self-healing, Robotics and automation.**

I. Introduction

An assumption in smart grid communications is that radios are immobile, mounted to existing power grid infrastructure such as transmission towers, upon poles, or near manholes for underground cables. It is often assumed that radios are integrated with intelligent electronic devices (IED), such as protection equipment. Even among stationary radio approaches, there are a myriad of possible technologies to choose from, including LTE, GPRS, 802.15.4 and Smart Utility Network (SUN) standards to WiMAX 802.16n and 802.16p for machine-to-machine operation, and 802.11 variants, including 802.11s and many others. In addition, delay tolerant networking approaches leverage vehicle-to-grid communications or any of a myriad of opportunistic networking approaches. The list of possible communication technologies and their performance characteristics is growing rapidly; the ability to simulate them all within the power grid is becoming a significant challenge. It is unlikely that the smart grid will standardize upon one approach, thus the ability to simulate all possible combinations of technologies to determine the optimal combinations technologies is becoming a significant challenge. A simpler approach to estimate performance is needed; such an approach is presented here.

The focus in this paper is upon fault detection, isolation, and recovery (FDIR), often considered "self-healing" capability [1]. The concept is to specify the power grid and communication network topologies as matrices, thus developing a generalized formula. The weighted (by customers) connectivity of each node in the power grid network topology, described in an adjacency matrix (PoA), determines its susceptibility to being isolated due to an electrical fault [2], [3], [4]. The communication network architecture, described in an adjacency matrix (CoA), provides the most efficient communication necessary to control the path for the least-connected (most-likely isolated) nodes of PoA. Conceptually, weakly connected nodes in PoA should tend to be strongly connected in CoA. However, it is also important to minimize connections in both PoA and CoA to reduce cost. The concept is to compute the eigenvector of the largest eigenvalue for both the PoA and CoA graph adjacency matrices. For robust and cost effective communication solutions, the corresponding eigenvectors should be anti-correlated.

Section II reviews electric power distribution network topologies. Section III considers the interaction with a communication network and reviews a simple algorithm for FDIR assuming a ring communication network. The goal is to advance beyond simple ring communication topologies and examine the impact of different power distribution and communication topologies. To this end, Section IV discusses a simple analytical model of the combined power and communication networks. In order to obtain quantifiable metrics, Section V reviews commonly-used FDIR metrics that capture both the duration and number of customers affected during a power outage. The main contribution is to derive the matrix form of previously defined scalar metrics. This allows both the power distribution network and communication network structures to be directly integrated into the definition of the metrics, thus enabling the dynamics of both network structures to be analyzed simultaneously. This result is extended to include stochastic fault analysis including false alarms and missed faults. From a communications perspective, the matrix definition facilitates analysis of the power distribution network impact upon load and routing on the communication network. Section VI notes that this analysis lays the foundation for network science in the form of spectral graph theory.

II. Distribution Configurations

The dynamics and topology of the distribution system impact the requirements for the communication network. Dynamics refers to the changes in topology due to faults; choice of topology has an impact upon faults and the potential use of tie switches to restore power to isolated segments. The simplest configuration is a radial distribution system [5].

A loop topology is slightly more complex and is shown in Figure 1. In this topology there are two substations, labeled

S. Bush is with GE Global Research, One Research Circle, Niskayuna, New York 12309 USA e-mail: (see http://www.amazon.com/author/stephenbush).

Manuscript received Mar 31, 2014; revised Mar 31, 2014.

0733-8716 (c) 2013 IEEE. Personal use is permitted, but republication/redistribution requires IEEE permission. See http://www.ieee.org/publications_standards/publications/rights/index.html for more information.

This article has been accepted for publication in a future issue of this journal, but has not been fully edited. Content may change prior to final publication. Citation information: DOI 10.1109/JSAC.2014.2332132, IEEE Journal on Selected Areas in Communications

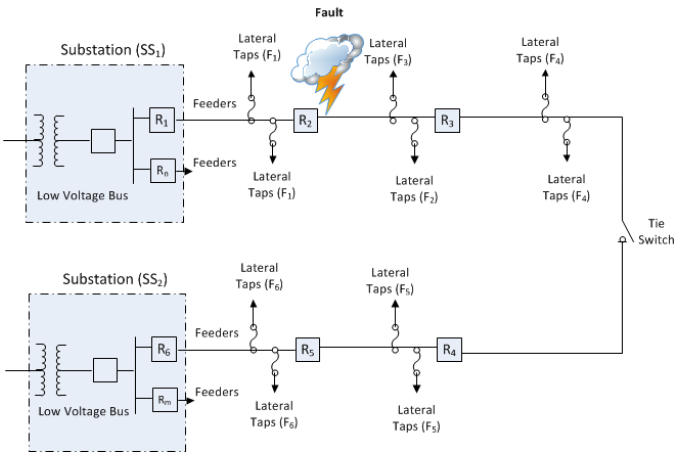

Fig. 1. A loop distribution network. There are two substations, SS_1 and SS_2. The tie switch is normally open but can close in order to share power between the upper and lower segments of the loop, increasing reliability. Efficient communication is required to ensure only the recloser upstream and closest to the fault opens, the tie switch closes, and that these events happen as quickly as possible in the correct order when the other substation has available power. A fault is indicated on the R_2 - R_3 segment.

SS_1 and SS_2. The tie switch is normally open. If necessary, the tie switch can be closed allowing power to flow across the upper or lower sections of the radial components of the loop system if needed. The next section reviews a simple communication algorithm for FDIR, which will be analyzed leading to a more complex matrix analysis in Section V.

Figure 2 illustrates simple, regular communication network topologies. There are many more interesting random or semi-random topologies that better optimize power reliability indices with less cost. The goal of this paper is to understand the impact of these topologies. Power distribution network topologies can also be more complex than simple radial or loop systems. Figure 3 illustrates a more complex power distribution topology. This particular 123-node feeder operates at 4.16 kV and contains multiple tie-switches. The goal of this paper is to explore how the communication network and power distribution network topologies interact to impact power system reliability.

III. The Algorithm

A summary of a simple FDIR algorithm described in [6] is provided as an example. A fault occurs in the location shown in Figure 1. Faults may occur anywhere between R_1 and R_6 in which an overcurrent is detected long enough to cause one of the reclosers to lockout. When the recloser opens, a bit is transmitted to two adjacent reclosers. Overcurrent sensing starts for the upstream device. The normally-open tie switch is closed to restore power to line sections without faults. The specific sequence of actions are explained in the following steps of the process:

1) The overcurrent sensors in R_1 and R_2 sense the fault
2) Recloser R_2 senses the overcurrent, performs its reclosing sequence and then locksout permanently, clearing the fault

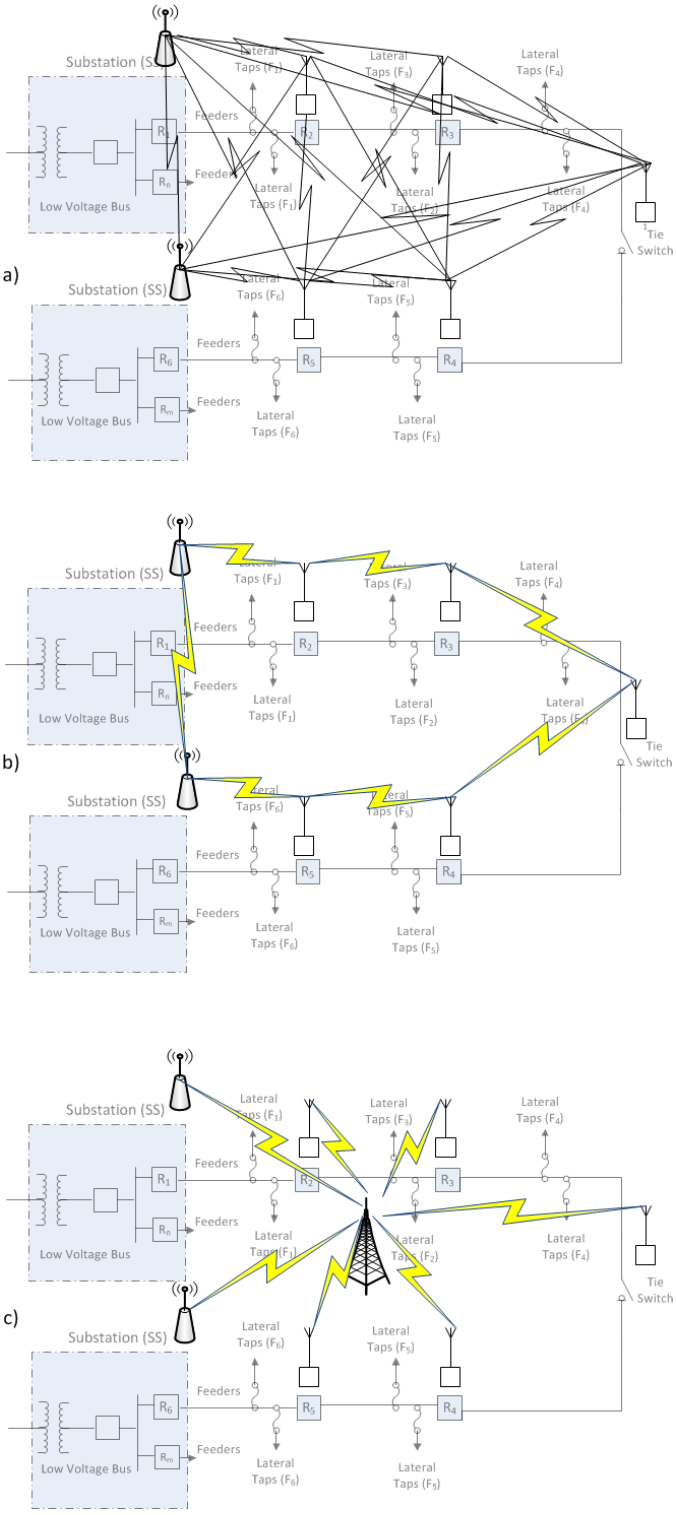

Fig. 2. An illustration of simple, regular network topologies for a simple loop distribution network. (a) mesh communication network topology, (b) ring, and (c) star. Other communication topologies include random or scale-free node degree distributions. The communication topology is represented by $\overline{\mathbf{CoA}}$ in Table I

3) Segments R_2 - R_3 and R_3 - tie switch are deenergized due to the lockout of R_2
4) R_2 transmits a message to R_1 and R_3 to indicate that it

0733-8716 (c) 2013 IEEE. Personal use is permitted, but republication/redistribution requires IEEE permission. See http://www.ieee.org/publications_standards/publications/rights/index.html for more information.

This article has been accepted for publication in a future issue of this journal, but has not been fully edited. Content may change prior to final publication. Citation information: DOI 10.1109/JSAC.2014.2332132, IEEE Journal on Selected Areas in Communications

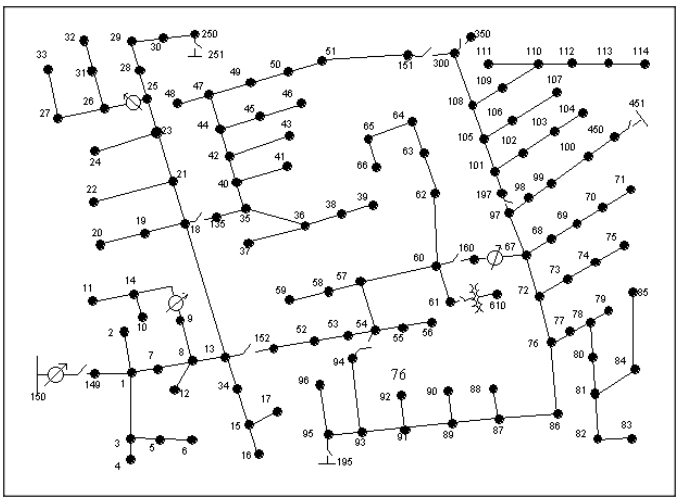

Fig. 3. The IEEE 123 Node Test Feeder (http://ewh.ieee.org/soc/pes/dsacom/testfeeders/index.html) illustrates a more complex distribution topology. Both the communication and power grid network topologies can be more complex. The power distribution topology is represented by $\overline{\mathbf{PoA}}$ in Table I.

has opened

5) The message transmitted by R_2 to R_1 is ignored in preference to the overcurrent sensing in R_1
6) When R_3 receives the transmitted message, it trips since no overcurrent has been sensed; when R_3 opens, this fully isolates the faulted section
7) R_3 transmits a message downlink to the tie switch
8) The tie switch, which is normally open, closes and restores power to the R_3 - R_4 section
9) If the tie switch were already closed, it would have relayed the message downstream until a normally open tie switch was found and closed

The Momentary Average Interruption Frequency Index (MAIFI) defined in Equation 6 is not reduced for affected customers if the outage is below the utility-defined threshold, typically five minutes today[7]. However, with advances in communication and automation, restoration times will decrease and indices will be computed more often. The total restoration time is the time for R_2 to lockout and for the tie switch to close. Opening R_3 is done in parallel with the previous steps.

A fault between R_3 and R_4 would behave similarly, except that the tie switch would remain open in order to isolate the faulted segment. The algorithm is summarized in Algorithm 1. The REQUIRE statement indicates a state that must exist, such as an overcurrent condition or reception of a bit from another node; *nearest-fault-neighbor* indicates a node is an immediate neighbor of a faulted segment; *not-a-tie-switch* indicates a node is not a tie switch, while *tie-switch* indicates a node is a tie switch. The algorithm assumes a ring communication topology. A star or mesh topology would require either a logical ring structure or a modification of the algorithm to include ability to address specific nodes. The next section introduces an analysis of the impact of communication on performance.

Algorithm 1 Recloser Algorithm for Ring Communication

Require: overcurrent-sensed:
  send bit to immediately adjacent neighbors
Require: bit-received:
  if overcurrent-sensed **then**
    ignore bit
  end if
  if nearest-fault-neighbor AND overcurrent-not-sensed AND not-a-tie-switch **then**
    open and pass bit around ring
  end if
  if not-a-tie-switch **then**
    pass bit around ring
  end if
  if tie-switch AND not-nearest-fault-neighbor **then**
    close tie switch
  end if

IV. A Simplified Scalar Analysis

This section considers a simple scalar analysis that will be extended to matrix form in the next section. While there has been a tendency to view smart grid radios as being embedded within stationary intelligent electronic devices resulting in relatively low variation in channel performance, this is not the case in reality. Trees and vegetation change throughout the year, vehicles reflect the signal, and there are numerous other forms of potentially varying clutter at pole height. The challenge with such an architecture is that radios reside at a relatively low height and non-optimal locations compared to cellular radio towers. They are subject to fading, which is attenuation of the signal strength due to both reflection from objects along the radio wave propagation path and shadowing, caused by objects obstructing radio wave propagation. Fading for non-mobile radios can be mitigated by using different types of diversity, either in time, frequency, or space. For example, adding channel coding, which requires additional overhead, transmitting repeatedly until the information is received, transmitting along multiple frequencies, or transmitting along multiple paths. The problem with these approaches is that they reduce the potential available bandwidth and require more expensive radios and more complex protocols.

A potentially simpler approach to mitigating fading is to allow one degree-of-freedom of motion as illustrated in Figure 4. This motion can allow radios or more specifically, their antennas, to move into optimal position to avoid fading. The advantages include the ability to achieve and maintain excellent connectivity throughout the wireless communication system. The same technique can be applied on transmission lines, however, the height of transmission towers is such that they are less susceptible to fading. Automated power line inspection and repair equipment, including power line crawling robots, have been developed for both the eclectic power transmission and distribution systems [8], [9], [10], [11]. Communication has always been considered an ancillary service to the function of the robots' main task. Here, the mobile radio has the primary function of mitigating fading

0733-8716 (c) 2013 IEEE. Personal use is permitted, but republication/redistribution requires IEEE permission. See http://www.ieee.org/publications_standards/publications/rights/index.html for more information.

This article has been accepted for publication in a future issue of this journal, but has not been fully edited. Content may change prior to final publication. Citation information: DOI 10.1109/JSAC.2014.2332132, IEEE Journal on Selected Areas in Communications

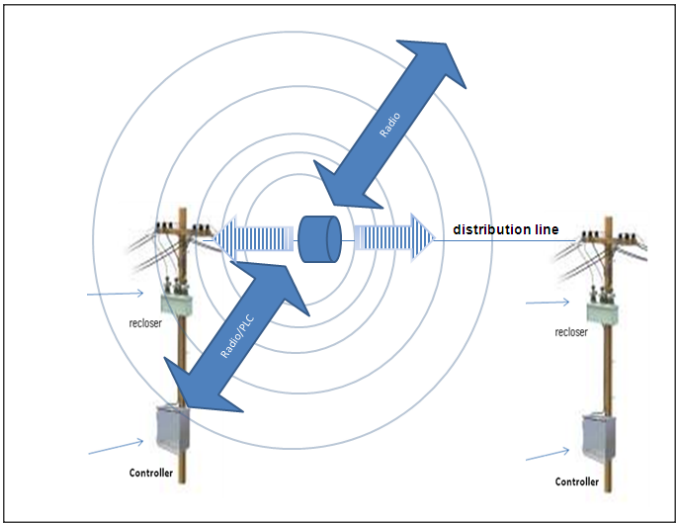

Fig. 4. The antenna and/or radio moves along the power line in order to improve multihop radio reception throughout a power distribution network. This generates a variable communication topology dependent upon ground clutter, but constrained to node positions along the underlying power distribution network topology graph edges.

for smart grid power distribution communication. Depending upon cost and benefit, nothing prevents the device from incorporating sensing and control elements along with its fading mitigation function. The concept comprises wireless radios or antennas mounted upon power line crawler devices capable of autonomous movement along the power line in order to optimize radio communication. The robotic crawler device is an inexpensive hollow cylinder placed around the power line, such that it cannot be easily dislodged from the power line, and utilizes any of a variety of mechanisms to propel itself along the power line. These could include, but are not limited to, an on-board motor with a wheel that grabs the power line and rotates to move the entire unit to magnetic field levitation and propulsion using the power line's electric and magnetic field properties. If the entire radio is placed on-board the robot, then transmission of information from the radio to stationary devices on the grid may utilize the power line as a waveguide in the form of power line carrier. Alternatively, only the radio's antenna need be placed on the robotic unit. In this case, the radio remains fixed within or near a recloser for example, and the antenna adjusts its position on the power line in order to improve communication. The distribution radio system is comprised of many mobile power line radios resulting in a communication network topology generated by the underlying power line topology.

The goal is to consider generalized characteristics for topological analysis. The impact of a fault depends upon the distribution of customers to each feeder and the segment upon which a fault occurs. Assume customers are uniformly distributed along feeders. For a completely automated restoration system, the restoration time is dependent upon fault detection time and the number of message transmissions required to restore power. Let the number of approximately one-kilometer segments between reclosers be s. There will be N/s customers on each segment where N is the total number of customers. A simplifying assumption is that the likelihood of a fault is proportional to the length of a power line segment. A longer segment will be more likely to suffer a fault given its greater exposure to the environment. For this simple analysis, assume that all lengths are equal. Also assume that the communication network is utilized to independently verify a fault sensed by a time-current curve. Given a uniform likelihood of a fault on any segment, there are $s/2$ reclosers to check on average, that is, $s/2$ transmissions are required to verify that the closest recloser to the fault has been identified. A binary search would yield $\lceil \log_2 s \rceil$ exchanges. If a tie switch is required in the case of a loop, then an additional transmission is required to close the tie switch. All customers downstream of a fault in a radial configuration will lose power. Thus, the mean number of customers without power after a fault given these simplified assumptions is $s/2 \times N/s$, or $N/2$. Assuming a constant number of users N, a small number of feeders and segments s implies quick communication and coordination while a large s implies the ability to isolate the line closer to the fault and keep more customers on line. Thus, there is an optimal value of s given these tradeoffs when designing the distribution system.

Using the process given in Algorithm 1, consider the number of transmissions, load, and time to resolve a fault given the size of the distribution network. Assume a ring network in which messages must flow sequentially through distribution devices along the ring. In other words, distribution devices forward messages around the ring until they reach their destination. This is in contrast to a fully connected mesh network in which any node may connect to any other node within its transmission range. The number of transmissions required is the number of nodes from the lockedout recloser R_f to tie switch R_t as shown in Equation 1 assuming messages are relayed by each node along the path.

$$n_t = R_t - R_f + 1 \tag{1}$$

The load is simply the number of transmissions n_t of GOOSE messages (defined in IEC 61850-7) of length 123 bytes with an additional 176 bytes of RSA encryption shown in Equation 2.

$$l = n_t(123 + 176)8 \tag{2}$$

Total latency is simply load divided by total bandwidth for each message plus the time it takes for the reclosers to process each message t_r shown in Equation 3. The protocol requires reliable communication; η is the efficiency of Go-Back-N Automatic Repeat reQuest (ARQ). The efficiency is governed by the size of the Go-Back-N ARQ window, which should equal the delay-bandwidth product of the channel, and the probability of a PDU error, which is based upon both wireless physical transmission errors and congestion within the network. The efficiency of Go-Back-N is approximated by Equation 4 where N is the window size and P is the probability of PDU error.

$$d = \left(\frac{l}{B\eta} + n_t \right) t_r \tag{3}$$

In this simplified analysis, it is assumed that the physical channel is perfect and congestion is proportional to the traffic

0733-8716 (c) 2013 IEEE. Personal use is permitted, but republication/redistribution requires IEEE permission. See http://www.ieee.org/publications_standards/publications/rights/index.html for more information.

This article has been accepted for publication in a future issue of this journal, but has not been fully edited. Content may change prior to final publication. Citation information: DOI 10.1109/JSAC.2014.2332132, IEEE Journal on Selected Areas in Communications

load. The raw physical layer bandwidth is B and η accounts for retransmission overhead.

$$\eta \equiv \frac{1}{1 + \frac{NP}{(1-P)}} \tag{4}$$

From Equation 1, n_t is the number of segments between the faulted segment and the tie switch in a loop distribution system. Thus, n_t is the number of segments that lose power until the tie switch is closed. This will later be tied directly to SAIFI metrics in order to determine the performance of the communication system in terms of outage duration.

The effective bandwidth is the actual bandwidth available for message transmission, after the bandwidth has been reduced by all protocol overhead and physical errors. There is a subtle tradeoff: if protection device operation time is long, there is less load on the network resulting in better network performance. As protection device times become shorter because the devices operate faster, they also increase load on the communication network, which can lead to congestion and retransmission, potentially increasing transmission time.

V. Performance Metrics

Performance metrics have been designed to quantify the impact of faults on the customer base [12]. The System Average Interruption Duration Index (SAIDI) is the sum of all customer interruption durations divided by the number of customers as shown in Equation 5.

$$SAIDI \equiv \frac{\sum r_i N_i}{N} \tag{5}$$

The index i is a load point and r_i is the average restoration time at load point i. MAIFI is similar to SAIDI except that it defines the customer impact in terms of the number of "momentary" outages, where the length of a moment can be arbitrarily defined. Thus, MAIFI is the number of interruptions greater than a specified duration divided by the number of customers as shown in Equation 6.

$$MAIFI \equiv \frac{\sum U_i N_i}{N} \tag{6}$$

The symbol U_i is the number of interruptions exceeding a given time at load point i.

To incorporate more detail into the analysis, consider the operational analysis in matrix form with the symbols defined in Table I. Matrices are accented with a bar and vectors with an arrow. Let there be r reclosers protecting r feeders. Let $\vec{N}$ be of dimension $(1 \times r)$ where each element of the vector is a feeder connection as shown in Figure 1. Let $\overline{\mathbf{F}}$ be a matrix of dimension $(r \times r)$ where each element indicates the presence or absence of a fault on the r power line segments represented by a zero or one $(0, 1)$. The index of the tie switch will be denoted by matrix $\overline{\mathbf{R}}$ of dimension $r \times r$, where a 1 indicates a tie switch connection and all other connections are 0. The interconnectivity of the electric power distribution network can be represented by a graph that is described by adjacency matrix $\overline{\mathbf{PoA}}$ of dimension $(r \times r)$. The graph is assumed to be undirected. A representation of the communication network

TABLE I
Summary of symbols used in the analysis.

Symbol	Dimension	Description
$\overline{\mathbf{PoA}}$	$r \times r$ matrix	Distribution adjacency matrix
$\vec{SS}$	$1 \times r$ vector	Substation vector
$\overline{\mathbf{CoA}}$	$r \times r$ matrix	Communication adjacency matrix
$\overline{\mathbf{R}}$	$r \times r$ matrix	Tie switch indicator matrix
$\overline{\mathbf{F}}$	$r \times r$ matrix	Fault indicator matrix
$\vec{\Psi}_{\mathbf{F}}$	$1 \times r$ vector	Isolated segments due to true faults
$\vec{\Psi}_{\mathbf{FP}}$	$1 \times r$ vector	Isolated segments due to false positives
$\vec{\Psi}_{\mathbf{FN}}$	$1 \times r$ vector	Isolated segments due to false negatives
$\vec{N}$	$1 \times r$ vector	Customers on each segment
$\vec{1}$	$1 \times r$ vector	All ones vector
$\vec{R}$	$1 \times r$ vector	Feeders restored after ties closed
$\overline{\mathbf{C}}$	$r \times r$ matrix	All pairs of shortest paths
$\overline{\mathbf{\Theta}}_{\mathbf{F}}$	$r \times r$ matrix	Prob of a true fault
$\overline{\mathbf{\Theta}}_{\mathbf{FP}}$	$r \times r$ matrix	Prob of false alarms
$\overline{\mathbf{\Theta}}_{\mathbf{FN}}$	$r \times r$ matrix	Prob of missed faults
η	scalar	Efficiency of ARQ
r_m	scalar (seconds)	Manual restoration time
r_t	scalar (seconds)	Automatic recloser time
f	scalar (recloser)	Faulted recloser (single fault)
t	scalar (switch)	Tie switch (single switch)

can be found in the connectivity matrix $\overline{\mathbf{CoA}}$, which is also of dimension $(r \times r)$ and indicates the interconnectivity and latency of the recloser radios.

The connectivity matrix $\overline{\mathbf{C}}$ indicates the total transmission latency from the node in the row index to the node in the column index. In other words, each element of the connectivity matrix represents the total communication latency in transmission between the row and column indices. $\overline{\mathbf{C}}$ can be derived from the adjacency matrix for the communication network, $\overline{\mathbf{CoA}}$. If there are n nodes then $\overline{\mathbf{C}}$ is derived from $\overline{\mathbf{CoA}}^n$, but with a difference in the manner of matrix multiplication. Specifically, the element-wise multiplication operation in the matrix multiplication is replaced with addition and the addition operation normally used in matrix multiplication is replaced with minimization, that is, taking the minimum value element. There is a latency of duration $\overline{\mathbf{C}}(f, t)$ in transmitting from the faulted segment f to the tie switch t.

The vector of feeders served during normal operation is derived in Equation 7. Vector and matrix dot product are indicated by '$\cdot$' in the equations in the remainder of this paper. Because $\overline{\mathbf{PoA}}$ is an adjacency matrix, Equation 7 yields the nodes traversed by tokens released from the corresponding nodes in $\vec{SS}$ after r hops, that is, the reachability from the substation.

$$\vec{SS} \cdot \sum_{i=1}^{r} \overline{\mathbf{PoA}}^i \tag{7}$$

The vector of feeders receiving power after a fault is determined by Equation 8. This is similar to Equation 7 except that faulted segments have been subtracted from the adjacency matrix. Note that $\vec{\Psi}$ is the vector defined in Equation 8 where nonzero values are replaced with zero, since they continue to receive power, and zero values are replaced with one, to

0733-8716 (c) 2013 IEEE. Personal use is permitted, but republication/redistribution requires IEEE permission. See http://www.ieee.org/publications_standards/publications/rights/index.html for more information.

This article has been accepted for publication in a future issue of this journal, but has not been fully edited. Content may change prior to final publication. Citation information: DOI 10.1109/JSAC.2014.2332132, IEEE Journal on Selected Areas in Communications

indicate that they are isolated from the distribution system.

$$\overrightarrow{SS} \cdot \sum_{i=1}^{r} \left(\overline{\mathbf{PoA}} - \overline{\mathbf{F}}\right)^i \tag{8}$$

It important to note that $\overline{\mathbf{F}}$ indicates *actual* faults, which makes the analysis simpler. A more complex version of this analysis could consider the details of fault sensing, for example, via a time-current characteristic curve. In this case, more time is required in order to detect smaller current faults; at any instant in time, there is the possibility for a false positive or false negative fault. This is considered later. The operation time r_t includes the time required to sense the fault. $\overline{\mathbf{R}}$ indicates the location of normally-open tie switches.

The vector of feeders restored by closing tie switches is shown in Equation 9. $\overline{\mathbf{R}}$ is an adjacency matrix, similar to $\overline{\mathbf{F}}$ except that it adds new links rather than subtracts them. Similar to $\vec{\Psi}$, $\vec{R}$ is an indicator vector in which nonzero values are replaced with zero and zero values replaced with one.

$$\overrightarrow{SS} \cdot \sum_{i=1}^{r} \left(\overline{\mathbf{PoA}} - \overline{\mathbf{F}} + \overline{\mathbf{R}}\right)^i \tag{9}$$

The total number of customers is shown in Equation 10. The inner product of $\vec{N}$ with the all ones vector results in the summation of all feeder customers.

$$\vec{1} \cdot \vec{N} \tag{10}$$

Putting together the terms describing both the power and communication networks from Equations 8, 9, and 10 to form SAIDI results in Equation 11, where $\vec{\Psi}$ and $\vec{R}$ represent the power distribution network and $\overline{\mathbf{C}}$ represents the communication network architecture. Note that $\overline{\mathbf{C}}$ is derived from $\overline{\mathbf{CoA}}$, the communication adjacency matrix, and $\vec{\Psi}$ and $\vec{R}$ are derived from $\overline{\mathbf{PoA}}$, the electric power distribution network adjacency matrix.

$$SAIDI = \frac{r_t \overline{\mathbf{C}}[f,t]\eta \vec{\Psi}_{\mathbf{F}} \cdot \vec{N} + r_m \vec{R} \cdot \vec{N}}{\vec{1} \cdot \vec{N}} \tag{11}$$

A small rearrangement of Equation 11 is shown in Equation 12.

$$SAIDI = \frac{\left(r_t \overline{\mathbf{C}}[f,t]\eta \vec{\Psi}_{\mathbf{F}} + r_m \vec{R}\right) \cdot \vec{N}}{\vec{1} \cdot \vec{N}} \tag{12}$$

The result in Equation 12 can be utilized to estimate performance for any size and topology of both electric power distribution and communication networks including multiple faults, assuming power and transport capacity are available. For a complex distribution network, it may be useful to find the optimal set of tie switches to close among a set of possible choices. In this case, the goal is to solve for the $\overline{\mathbf{R}}$ that meets a given a criteria, such as minimizing SAIDI. Rearrangement of Equation 9 is shown in Equation 13, in which $\overline{\mathbf{R}}$ is separated into its own summation.

$$\overrightarrow{SS} \cdot \sum_{i=1}^{r} \left(\overline{\mathbf{PoA}} - \overline{\mathbf{F}}\right)^i + \overrightarrow{SS} \cdot \sum_{i=1}^{r} \overline{\mathbf{R}}^i \tag{13}$$

The next section considers extending the analysis to probabilistic cases; faults are no longer deterministically defined in $\overline{\mathbf{F}}$, but rather probabilistically defined in $\overline{\mathbf{\Theta}}$.

A. Probabilistic interpretation

Equation 12, derived previously, may be used to examine the impact of setting time-current characteristic curves (TCC) in a probabilistic sense. The fault matrix $\overline{\mathbf{F}}$ may represent a probability of fault, based upon the magnitude and duration of overcurrent.

$\overline{\mathbf{\Theta}}_{\mathbf{FP}}$, $\overline{\mathbf{\Theta}}_{\mathbf{FN}}$ and $\overline{\mathbf{\Theta}}_{\mathbf{F}}$ are $(r \times r)$ matrices used to capture the impact of time-current characteristic curve settings. They represent the probability of a false positive, false negative, and true positive respectively for each protected segment. $\overline{\mathbf{\Theta}}_{\mathbf{FP}}$ indicates the probability of the relay opening when it should not, thus needlessly isolating customers. $\overline{\mathbf{\Theta}}_{\mathbf{FN}}$ indicates the probability of the relay failing to open when when a fault is present, thus damaging equipment and failing to properly open any tie switches that could have mitigated the isolated segments. $\overline{\mathbf{\Theta}}_{\mathbf{F}}$ indicates the probability of a true fault.

The false positive matrix $\overline{\mathbf{\Theta}}_{\mathbf{FP}}$ is treated similar to $\overline{\mathbf{F}}$, as it represents the probability of a fault, which may differ on each segment. Consider transforming these adjacency matrices to a probability vector $\vec{\Psi}$ of isolated links due to faults. The approach is to compute the probability of successful power transmission $1 - \overline{\mathbf{\Theta}}_{\mathbf{FP/FN/F}}$.

Let the elements of $\overline{\mathbf{\Theta}}_{\mathbf{FP/FN/F}}$ be the probability of the power line segment opening for any reason. Then $1 - \overline{\mathbf{\Theta}}_{\mathbf{FP/FN/F}}$ is the probability of not opening, which is only a true no fault condition. All other conditions (true positive–opening due to a real fault, false positive–opening for a false alarm, false negative–missing a real fault) cause open sequencing or an open condition to occur. Equation 14 represents the probability of a false positive over any path through the grid. Specifically, the first row shows the probability of a false positive from the substation to any point through the grid. This applies similarly to false negatives and the probability of true faults. This provides an indication of the probability of each segment being isolated due to true faults, missed faults and thus equipment damage, or false alarms and those needless isolation of a segment. Segments further from the substation will have a greater chance of becoming isolated simply because the longer distance affords more opportunity for faults to occur. Thus, we can now speak of probabilistically mitigating isolation. For example, assuming the first recloser is connected to a substation, the top row of the resulting matrix from Equation 14 yields $\vec{\Psi}_{FP/FN/F}$.

$$1 - \sum_{i=1}^{r} \overline{\mathbf{\Theta}}_{\mathbf{FP/FN/F}}{}^i \tag{14}$$

Equation 15 shows SAIDI given the probability of false positives and false negatives.

$$SAIDI = \frac{\left(r_t \overline{\mathbf{C}}[f,t]\eta \vec{\Psi}_{\mathbf{FP/FN/F}} + r_m \vec{R}\right) \cdot \vec{N}}{\vec{1} \cdot \vec{N}} \tag{15}$$

The complete equation for SAIDI is shown in Equation 16, where $d()$ is a function that takes the adjacency matrix and returns the connectivity, or distance, matrix and $z()$ takes a vector and replaces zero values with 1 and all other values

0733-8716 (c) 2013 IEEE. Personal use is permitted, but republication/redistribution requires IEEE permission. See http://www.ieee.org/publications_standards/publications/rights/index.html for more information.

This article has been accepted for publication in a future issue of this journal, but has not been fully edited. Content may change prior to final publication. Citation information: DOI 10.1109/JSAC.2014.2332132, IEEE Journal on Selected Areas in Communications

with zero.

$$SAIDI = \frac{\left(r_t d(\overline{\mathbf{CoA}})[f,t]\eta z(\overrightarrow{SS}\cdot\sum_{i=1}^{r}\left(\overline{\mathbf{PoA}}-\overline{\mathbf{F}}\right)^{i})\right)\cdot\overrightarrow{N}}{\overrightarrow{1}\cdot\overrightarrow{N}} + \frac{\left(r_m z(\overrightarrow{SS}\cdot\sum_{i=1}^{r}\left(\overline{\mathbf{PoA}}-\overline{\mathbf{F}}+\overline{\mathbf{R}}\right)^{i})\right)\cdot\overrightarrow{N}}{\overrightarrow{1}\cdot\overrightarrow{N}} \quad (16)$$

There are few items to note in the Equation 16. The structure of the communication adjacency matrix $\overline{\mathbf{CoA}}$) has a direct impact on the connectivity matrix $d(\overline{\mathbf{CoA}})$ and the latency of the route taken by the FDIR messages $d(\overline{\mathbf{CoA}})[f,t]$. The structure of the power grid adjacency matrix $\overline{\mathbf{PoA}}$ in conjunction with the fault matrix $\overline{\mathbf{F}}$ and tie switch matrix $\overline{\mathbf{R}}$ impacts the number of isolated segments.

There are competing goals indicated by $\overline{\mathbf{\Theta}}_{\mathbf{FP}}$ and $\overline{\mathbf{\Theta}}_{\mathbf{FN}}$: detect all faults as quickly as possible without initiating false alarms. An increase in both false positives and false negatives increases SAIDI. Segments that we can now quantify with high a probability of fault or isolation may receive more attention from collaborative communications.

Determining the probability of fault and isolation also allows a determination of the probability of events for reconfiguration within the FDIR process. Returning to the main theme of a coupled network system, namely: (1) the electric distribution network and (2) the communication network, the probability of a fault on the electric power distribution network determines the probability of a corresponding message being transmitted on the communication network. In the absence of a priori fault information, all electric power grid segments are equally likely to experience a fault, that is, the system is at its highest entropy and the communication network must correspondingly be designed to handle messages from any segment. As more a priori information about the likelihood of faults becomes available, the entropy decreases and the communication network can expect to dedicate more resources to the segments with higher probability of faults, which includes impacts on the physical communication topology and routing. The concept of predictability and network behavior is discussed in [13].

VI. Conclusion

This paper has developed a fundamental formula representing how the power distribution network and the communication network interact as a protection system. Using the analytical model derived in Equation 11, wireless network performance can be tied directly to the SAIDI performance metric in matrix form enabling eigenvalue analysis of network topological properties such as the strength of graph connectivity and likelihood of isolated graph components [14].

Figure 5 shows the impact of communication network architectures on SAIDI metrics for a loop distribution system using a surface with dimensions of SAIDI (seconds), protection size (reclosers), and fault location (recloser on faulted segment). These are results of a 12-node loop distribution system shown in Figure 2 with the tie switch at node six. Figure 5(a) shows a ring communication architecture. Figure 5(b) shows a star communication architecture. Figure 5(c) shows a mesh communication architecture. Figure 5(d) shows all three communication architectures simultaneously. The ring architecture shows the largest SAIDI values, which occurs for large networks when the tie switch is located relatively far from the fault. The mesh network shows the lowest latency with least variation due to the idealized mesh redundant links.

Future work will leverage the results in this paper to optimize the FDIR system by better understanding how the power distribution network impacts the communication network and how communication can best aid the distribution network.

Acknowledgment

The author would like to thank Michael Mahony (GE Global Research) for his help and support as well as Michael Thesing and Ken Caird from GE Digital Energy for their expert feedback and advice.

References

[1] S. F. Bush, S. Goel, and G. Simard, "IEEE Vision for Smart Grid Communications: 2030 and Beyond Roadmap," 2013.

[2] S. F. Bush, "Information Theory and Network Science for Power Systems," in *IEEE Vision for Smart Grid Communications: 2030 and Beyond*. IEEE Standards, 2013, ch. 5, pp. 128–161.

[3] S. F. Bush and S. Goel, "Graph Spectra for Communications in Biological and Carbon Nanotube Networks," *IEEE Journal on Selected Areas in Communications*, pp. 1–10, 2014.

[4] S. F. Bush, *Smart Grid: Communication-Enabled Intelligence for the Electric Power Grid*. Wiley-IEEE Press, 2014.

[5] T. Taylor, M. Marshall, and E. Neumann, "Developing a reliability improvement strategy for utility distribution systems," in *2001 IEEE/PES Transmission and Distribution Conference and Exposition. Developing New Perspectives (Cat. No.01CH37294)*. IEEE, 2001, pp. 444–449.

[6] G. Hataway, T. Warren, and C. Stephens, *Implementation of a High-Speed Distribution Network Reconfiguration Scheme*. IEEE, 2006.

[7] "IEEE Guide for Electric Power Distribution Reliability Indices," *IEEE Std 1366-1998*, pp. 1–21, Apr. 1999.

[8] B. Jiang and A. Mamishev, "Robotic Monitoring of Power Systems," *IEEE Transactions on Power Delivery*, vol. 19, no. 3, pp. 912–918, Jul. 2004.

[9] R. A. Roncolatto, N. W. Romanelli, A. Hirakawa, O. Horikawa, D. M. Vieira, R. Yamamoto, V. C. Finotto, V. Sverzuti, and I. P. Lopes, "Robotics applied to work conditions improvement in power distribution lines maintenance," in *2010 1st International Conference on Applied Robotics for the Power Industry (CARPI 2010)*. IEEE, Oct. 2010, pp. 1–6.

[10] S. Montambault and N. Pouliot, "About the future of power line robotics," in *2010 1st International Conference on Applied Robotics for the Power Industry (CARPI 2010)*. IEEE, Oct. 2010, pp. 1–6.

[11] D. Elizondo, T. Gentile, H. Candia, and G. Bell, "Overview of robotic applications for energized transmission line work Technologies, field projects and future developments," in *2010 1st International Conference on Applied Robotics for the Power Industry (CARPI 2010)*. IEEE, Oct. 2010, pp. 1–7.

[12] R. M. Cheney, J. T. Thorne, G. Hataway, and A. P. Co, *Distribution single-phase tripping and reclosing: Overcoming obstacles with programmable recloser controls*. IEEE, Mar. 2009.

[13] S. F. Bush and N. Smith, "The Limits of Motion Prediction Support for Ad hoc Wireless Network Performance," *Arxiv preprint cs/0512092*, pp. 27–30, Dec. 2005. [Online]. Available: http://arxiv.org/abs/cs.NI/0512092

[14] S. F. Bush, "Scale-free routing topology for a power network," *US Patent 20130003603 A1*, 2011. [Online]. Available: https://www.google.com/patents/US20130003603

0733-8716 (c) 2013 IEEE. Personal use is permitted, but republication/redistribution requires IEEE permission. See http://www.ieee.org/publications_standards/publications/rights/index.html for more information.

This article has been accepted for publication in a future issue of this journal, but has not been fully edited. Content may change prior to final publication. Citation information: DOI 10.1109/JSAC.2014.2332132, IEEE Journal on Selected Areas in Communications

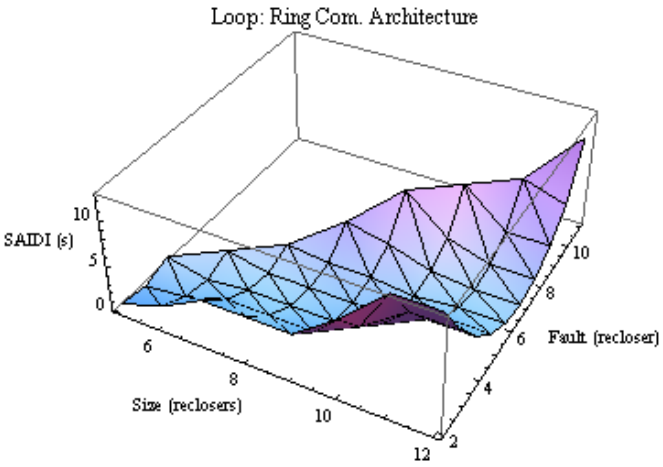

(a) The SAIDI surface is calculated for communication that follows a loop topology. Faults closer to the tie switch result in faster operation resulting in the concave shape.

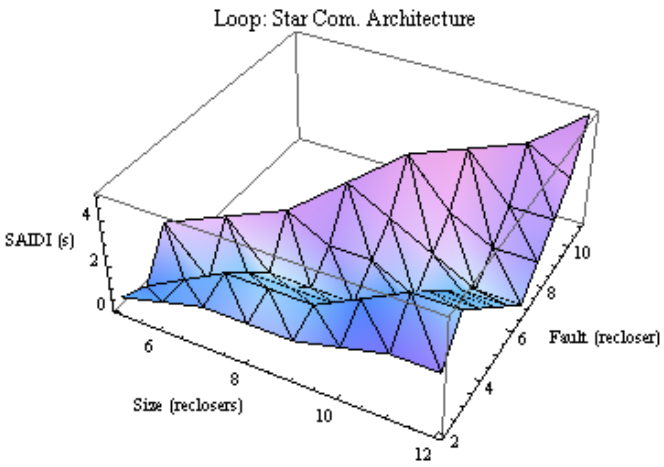

(b) The SAIDI surface is calculated for communication that follows a star topology. SAIDI values are improved while faults closer to the tie switch are faster to heal.

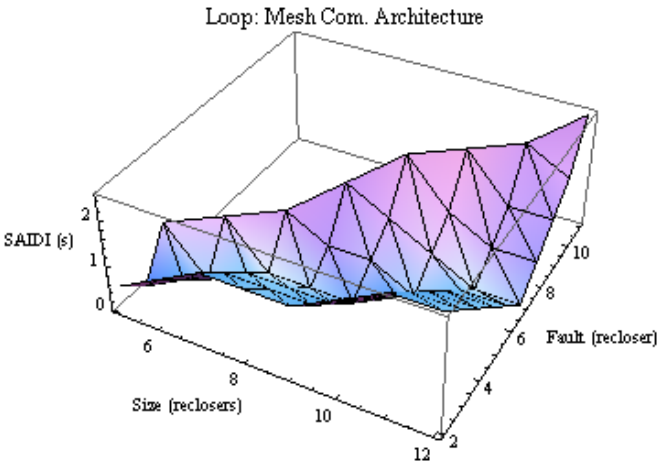

(c) The SAIDI surface is calculated for communication that follows an ideal mesh topology. The SAIDI surface is significantly flattened.

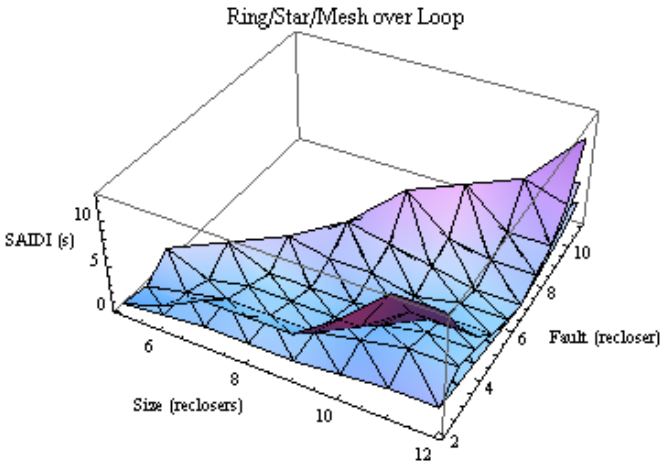

(d) The SAIDI as a function of size of the distribution system in segments and the location of the fault segment for ring, star, and mesh communication architectures. The mesh surface is located at the bottom and is the smoothest, indicating least variance with distribution size and location of fault due to the idealized mesh redundant links.

Fig. 5. (a–d) The impact of different network architectures are shown on the SAIDI value for a loop distribution network. Size is the number of segments, where each segmented is protected by a recloser. A fault can only occur on an existing segment, thus the surface forms a triangular surface. SAIDI dips in the center for segments located closer to the tie switch (node size).

Stephen F. Bush (M'03-SM'03) received the B.S. degree in electrical and computer engineering from Carnegie Mellon University, Pittsburgh, PA, the M.S. degree in computer science from Cleveland State University, Cleveland, OH, and the Ph.D. degree from the University of Kansas, Lawrence.

He is a Senior Scientist at General Electric Global Research, Niskayuna, NY. He has authored several books: Smart Grid: Communication-Enabled Intelligence for the Electric Power Grid (ISBN: 978-1-119-97580-9, 576 pages, March 2014, Wiley-IEEE Press), Nanoscale Communication Networks (Norwood, MA: Artech House, 2010) and coauthored a book on active network management entitled Active Networks and Active Network Management: A Proactive Management Framework (New York, NY: Kluwer Academic/Plenum Publishers, 2001).

Dr. Bush volunteers his time as Founder and Past Chair of the IEEE Emerging Technical Subcommittee on Nanoscale, Molecular, and Quantum Networking and is currently Chair of the IEEE 1906.1 standards working group on nanoscale communication networks as well as touring as an IEEE Distinguished Lecturer on the smart grid and nanoscale communication networks.

0733-8716 (c) 2013 IEEE. Personal use is permitted, but republication/redistribution requires IEEE permission. See http://www.ieee.org/publications_standards/publications/rights/index.html for more information.